



Article Processing Dates: Received on 2023-07-18, Reviewed on 2023-08-17, Revised on 2023-09-04, Accepted on 2023-10-29 and Available online on 2023-10-30

## Experimental study fluidized bed reactor using number hole 8 to see distribution gas fluid pressure

Eswanto\*, Riza Refaya Pinem, Suprpto

Mechanical Engineering, Universitas Negeri Medan, Medan 20221, Indonesia

\*Corresponding author: [eswanto@unimed.ac.id](mailto:eswanto@unimed.ac.id)

### Abstract

Innovations related to fluidization systems using fluidized bed reactor still need to be developed to improve the fluidization process services for particles to produce the right fluid pressure in certain fluidized bed spaces that are currently operating. In this research, the pressurized fluid in question is air sourced from a compressor which has been arranged in such a way. The research aims to obtain information regarding the characteristics of bubbles resulting from the air pressure process pressing fluidized system particles. The research method was carried out by experimenting with testing a fluidized bed reactor as a test model in the form of 8 holes, providing air pressure from the compressor, and then observing the characteristics visually. The results of this visually documented research have been carried out and obtained. By using the number of holes 8 with height silica sand inserted to the height of 25 cm, which is measured from the beginning of the hole plate before pressure is applied. After being given high pressure the bed increased to 27.6 cm, the highest bubble diameter was obtained at the input air pressure of 8 bar, which was 3.9 cm, with bed silica sand produced at 26.1 cm, where the bubble condition began to appear after the 9<sup>th</sup> second. Other characteristics also obtained reactor temperature of 25.45°C where this condition is the smallest when compared to other pressure input results, this is because the small input pressure causes the temperature to be low, while the large pressure input temperature becomes higher due to many factors, including friction between silica sand, silica sand collisions, and faster movement of particle material.

### Keywords:

Fluidized bed, hole, reactor, silica particle, gas.

### 1 Introduction

The scientific discussions among researchers related to the reactor of fluidization models are very interesting and need to be taken seriously, where fluidization is a phenomenon of fluid properties in the form of solids that change in the reactor space that has been designed to produce fluidized fluid. When viewed from the theory, the reaction that occurs in the fluidization system through the reactor is called a fluidized bed [1]. The fluidized bed is a container in the form of solid particles that are flowed by fluid from the bottom. In the industrial world today fluidized bed has been applied in various types of reactor such as in the drying process of a product, combustion system, gasification, coating and others [2][3].

The advantage of the fluidization process is that the fluid properties that can be flowed from solid operations can be continuous [4] because it can lift the grain particles until they float

and the contact surface area becomes very large so it is very effective, circulation of fluidized solid grains can allow large heat transfer in the reactor chamber with minimal disturbance [5][6]. Research related to fluidized bed in recent decades has shown that the characteristics of the bubble produced are influenced by geometry parameters, diameter, number of holes, distance between holes, and the arrangement or configuration of holes in the distributor [7]. In theory, the factors that affect the minimum speed of fluidization are the nature of the particles, the nature of the fluid as a fluidization medium and the height of the bed. The shape of the distributor influences the minimum velocity of fluidized bed fluidization [8].

Research has been conducted on the fluidized bed, which is related to the expansion of the bed to determine the multi-bubble behavior of the fluid in the form of micro-solid fluid, where the results show that the contraction of the lower bed appears due to the lower velocity of the distributed liquid or for the gas velocity must be higher [9]-[11]. The characteristics of bubbles are also determined by the existence of probabilities and of course, there will be differences between fluids in liquid and solid form [12].

On the other hand, the effect of variations in air velocity on the performance of the fluidized bed gasifier by using a nozzle as an air distributor has a different characteristic impact on each of the data results obtained. The results of this study indicate that variations in air velocity greatly affect the temperature of the reactor, the amount of heat generated and the resulting effective flame time [13].

Research related to flow characterization in a bubbly fluidized bed reactor produced due to fluctuating gas pressure has also been conducted. The research aims to analyze the characteristics of results of input pressure applied fluctuatingly in a fluidized bed. Other parameters observed such as the effect of superficial gas velocity, bed section placement, particle size and pressure probe position to obtain flow behavior have been conditioned accordingly. In general, the results obtained show that the flow behavior at the bottom of a fluidized bed reactor is more complex than at the top, this is because bottom of a fluidized bed reactor the particle that is first exposed to fluid flow pressure [14]-[16].

Researchers who are concerned in this research field examined the experimental study of the non-uniform bubble rise process in the fluidized bed reactor in 2017 using a permanent bed with an alternating or zig-zag hole arrangement and the largest hole size in the middle of the bed, where it can be reported conclusion of this study is that the process of non-uniform air bubble rise occurs in the inner fluidization layer, resulting in large bubble generation [17]. Bubble distribution, growth and residence time at the transition from uniform to non-uniform bubble rise [18][19].

E. Cano-Pleite, et. al, conducted an experimental study on the motion of solids around isolated bubble rising vertically vibrating bed sections and concluded from their research results showed the presence of bubbles in this system disrupts the compression and expansion behavior thus eventually affecting the velocity of expansion waves moving up the bed, however, direct comparison of the experimental results with potential flow model revealed that this model is still valid for prediction of solid velocity around bubble in a vertically vibrating fluidized bed [20].

Research using the fluidized bed model Inverse Liquid-Solid Circulator Fluidized Bed (ILSCFB) has been carried out by previous researchers. The circulating fluidized bed consists of a downer with an inner diameter of 7.6cm and a height of 5.4 m, and an upcomer with an inner diameter of 20cm. The results of this research show that single particle forces move freely and sometimes reverse circulation occurs [21]. This study investigated the potential use of four different natural ores namely: olivine, bauxite, feldspar, and silica sand, as base materials for polyethylene vapor cracking in a bubbling fluidized bed reactor at 750°C. Steam performance is measured by product, conversion, and distribution. Olivine and feldspar show higher yields of

olefins, while silica sand and bauxite show higher yields of aromatics [22]. The results show the fundamental differences between air and oxyfuel conditions in a real combustion environment, and also reveal the differences between the sorbents. In general, a significantly higher SO<sub>2</sub> capture ratio was reached in oxyfuel conditions. At Ca/S equal to 5, it is possible to reach the SO<sub>2</sub> capture as high as 98% in oxyfuel mode. The BET surface of the sorbent is important mainly at lower Ca/S molar ratios. The difference in SO<sub>2</sub> capture between the sorbents is below 10% relative at Ca/S molar ratio 3 and it further decreases with increasing Ca/S ratio [23]. Analysis of the pressure overshoot provided insight into the hysteresis behavior that is commonly observed in micro-fluidization experiments. Here we believe that liquid bridges form in the bed via the absorption of humidity from the atmosphere over time. This suggests that particle-particle forces rather than wall effects are the dominant factor that influences the fluidization quality. Through subsequent analysis of wall effects by considering the ratio of pressure overshoot to buoyant weight, we identified that pre-fluidization drastically improved the fluidisation quality, which we think removes said liquid bridges [24]. Numerous experimental and theoretical investigations have been conducted, often focussed on minimum bubbling and fluidization velocities and bed expansion [25]. Collectively, these investigations have revealed that micro fluidized beds possess several unique features in comparison to ‘macro’ fluidized beds. Because micro-fluidized beds possess a higher surface area to volume ratio than ‘macro’ beds, friction between the bed and walls becomes more significant, [26-28].

In the industrial world, there are still many problems that need to be solved related to this fluidized bed, therefore fluidized bed research must continue to be improved, one of which is less efficient fluidization, so this fluidized bed research focuses on the characteristics of bubble produced as development in reactor industry fluidized model. The purpose of the research is to obtain information related to the characteristics of bubbles generated from the process of fluidized system.

## 2 Research Methods

Fig. 1 is a complete installation of research equipment used in the data collection process after calibration. Instrument calibration, especially for instruments installed to obtain research data, where the permitted error for all is below 10% depending on the condition of each measuring instrument. This research was carried out experimentally in the form of a test using 8 holes to see

the gas fluid pressure distribution in the fluidized bed reactor. Compressed air is supplied to the fluidized bed reactor through the compressor by adjusting the speed of air flowing through connecting hoses by first ensuring that there are no leaks. The speed of flowing air is measured with a special air rotameter with a wiebrock type with a capacity of 10-100 l/min air. The air entering the reactor at the bottom or what is called the bed, pressure is measured using a pressure switch that has been installed connected to a hose on the wall of the bed with a capacity of 0 to 12 bar, but in this research the air pressure is conditioned to maximum of 8 bar with variation in intake every 2 bar, where the entire reactor chamber is made of glass with thickness of 5 mm, while the pressure in compressor tube measured with pressure gauge which is also attached to the wall of air compressor tube. A thermocouple type K with a temperature range of 0°C to 1024°C was also installed to ensure the measurement of the temperature of the fluidized bed reactor being tested. The data collection process was carried out by varying the air pressure entering the reactor chamber at the bottom of the bed, namely 4 bar, 6 bar, and 8 bar. The data recording time is carried out when the condition of the reactor room is in constant condition, namely on average every 3 minutes for each measurement. The data has been obtained from the measurement results and then processed, starting from the conversion of units measurement, raw data calculations, conversion to graphical form to analysis of the results data processing.

In general, the research process in collecting this data has been carried out by experimental methods on the tool shown in Fig. 1, the test model setting is placed at number 6 (Fig.1(a)) while when collecting data the compressor air pressure is set at number 10. The final stage of this research makes a correlation with the results of research related to previous research, especially those that are close to the basic theory and its relation to standard feasible use or feasible application with optimal performance. If described in general, the implementation process field consists initial preparation process, implementation process, analysis, and completion.

In this study, we chose to use 8 holes because to obtain information on the characteristics of the bubbles produced, several references have been obtained using a larger hole size than that which still produces less stable bubble fluctuations, and vice versa if the number is below 8 holes, the pressure is large but takes a long time. the formation of a fluidized air bubble.

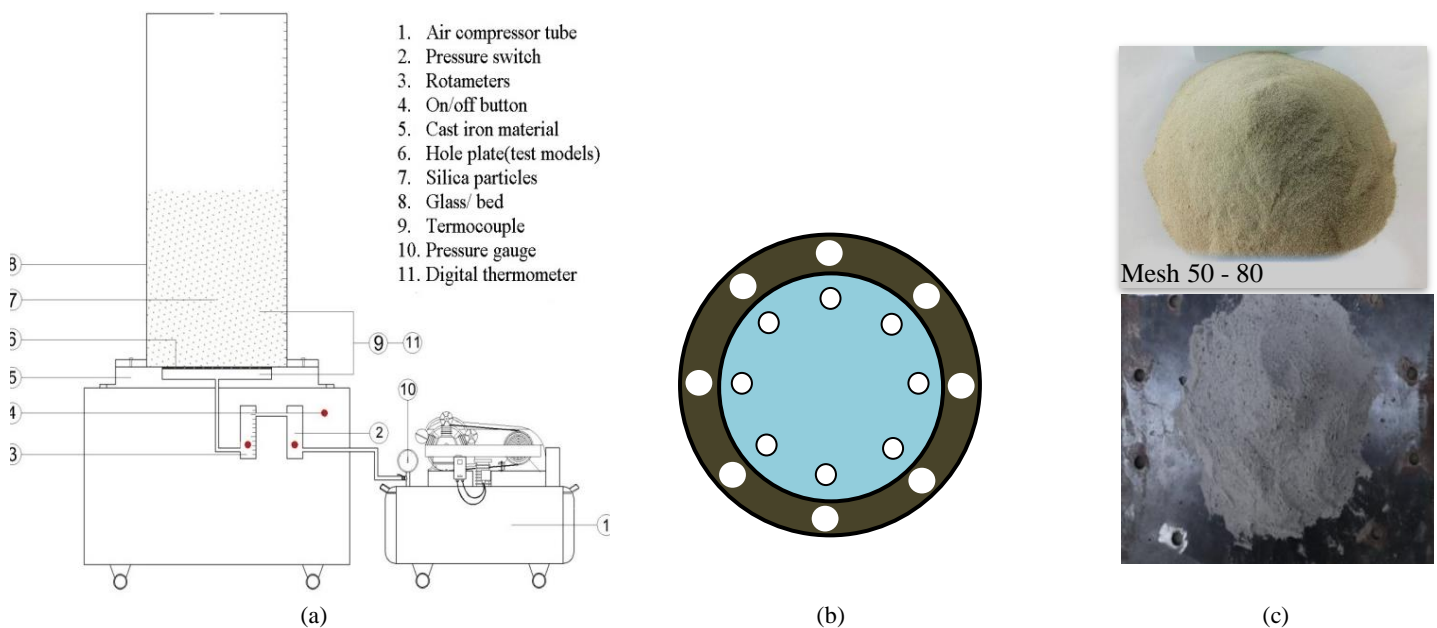


Fig. 1. Set up of fluidized bed test apparatus. a) Complete installation of fluidized bed reactor test equipment. b) Testbed model with 8 holes. c) Silica sand particle material.

Table 1. Specifications of measuring instruments used in this research

Measuring tools and equipment	Units	Specifications
Compressor power	Hp	1,5
Thermometer	Ohm	k/J Pt 100, 4 channels
Thermocouple type K	°C	0 until 1024 maks
Pressure gauge	bar	0 until 12 maks
Pressure switch control		2 until 8 maks
Rotameters	l/min	10 until 100 maks

In actual conditions, to complement and facilitate the uniqueness of this study, detailed specifications for the research tool are presented in Table 1 and test parameters in Table 2. Operational conditions were tested to obtain data in accordance with research standard. Before testing the research equipment, it is calibrated based on the applicable measurement rules.

This research has been carried out using silica sand as the working fluid in a fluidized system, which was chosen because the silica material has a relatively light mesh size and weight, is easy to spread from a solid state and can combine with various similar or dissimilar materials in the framework for the system fluidized. Apart from that, silica sand was chosen because it can conduct stable heat in the fluidized reactor chamber, so that the particle fluidization process in the reactor runs continuously which can stabilize the efficiency of the fluidized reactor.

### 3 Results and Discussion

In this study, what was varied was the inlet air pressure through the compressor, namely 4 bar, 6 bar, and 8 bar using an 8-hole test model where the air distributor exits. The data results were obtained visually from photographs and recorded manually, then the data processing has been presented in full in the results section of this article. In processing the data, it is taken directly from a visual photo and then the image is enlarged so that the size can be immediately seen from the ruler rollers installed on the left and right sides of the reactor, so that no equations are used in calculating the size of the air bubbles produced.

#### 3.1 Visual Characteristics of Babble at Pressure 4 Bar

In this study, the results obtained after analyzing data are then presented in graphical form, these conditions are used to understand and facilitate concise and structured presentation at a test pressure of 4 bar. The results of this study show that at pressure 4 bar, the average temperature reactor is 25.45°C with babble test material using silica sand material, the time of taking data on the rising bubble starts at the 3<sup>rd</sup> second, because at that time the babble starts to rise, then continues taking data at the 6<sup>th</sup> second and 9<sup>th</sup> second. To normalize the babble so that it can be seen visually, the babble fluctuation is left constant for 2 minutes, and so on in the experimental process that has been done. The sand height in this experiment is 25 cm measured from the beginning hole plate before pressure was applied. After the pressure is applied, the height of the bed rises to 27.6 cm, the diameter bubble produced at the 9<sup>th</sup> second an average of  $\varnothing = 3.9$  cm with silica sand overlay of 26.1 cm, when viewed visually in Fig. 2(a) the bubble formed are still very small, starting with the rise in the middle reactor that has been filled with silica sand and then being pushed up at the time of 5<sup>th</sup> second, then the babble rises higher and form like wave as shown in Fig. 2(b).

Table 2. The test parameters used in this study

Test parameters	Units	Research range
Fluidized bed reactor	cm	25 × 10 × 70
Hole diameters (d)	mm	2
Air pressure (P)	bar	4, 6 and 8
Number of holes (z)	hole	8
Thick acrylic	mm	5
Silica sand	mesh	70

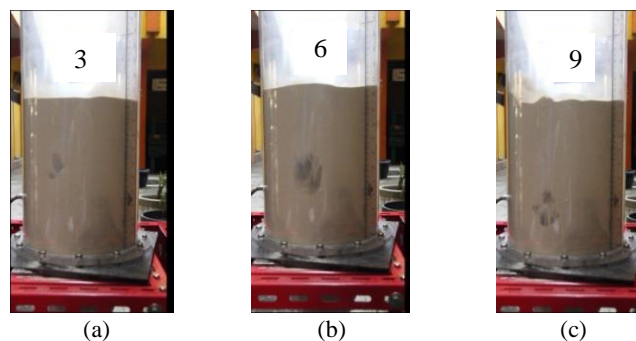


Fig. 2. Visual photographs of bubble fluctuations at pressure 4 bar. a) Visual babble at second 3. b) Visual babble at second 6. c) Visual babble at second 9.

#### 3.2 Visual Characteristics of Babble at Pressure 6 Bar

Fig. 3 is a visual photo taken at 6 bar air pressure input data entered through the bottom of the fluidized bed reactor. This study also still uses silica sand as a fluidization medium for the fluidized model, where the test data starts from the time of bubble rise that occurs in the reactor room. In this study, it was obtained that the fluidization bubbles began to rise at the 3<sup>rd</sup> second, 6<sup>th</sup> second and 9<sup>th</sup> second, where each increase at different times showed that the babble fluctuations were also different in size, both terms of height and diameter of bubble fluctuations. The height of silica sand used in this experiment was 25 cm measured from the beginning of the hole plate before pressure was applied. After pressure is applied, the height of the bed rises to 28.5 cm, the diameter bubble produced at 9 seconds is 3.1 cm measured under constant conditions, while the silica sand overlay is obtained at 27.3 cm with the average temperature of fluidized bed reactor is 27.75°C.

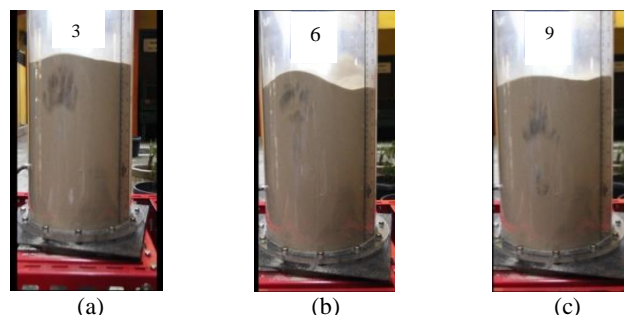


Fig. 3. Visual photographs of bubble fluctuations at pressure 6 bar. a) Visual babble at second 3. b) Visual babble at second 6. c) Visual babble at second 9.

From the explanation in Fig. 2 and Fig. 3, of course, this can confirm that the various influences and characteristics of bubbles resulting from fluidization occur due to several forces that support the particle material as well as input air pressure from the compressor. This condition has also been stated by several previous researchers, namely Z. Fu et. al. and W. Yoshimori et. al., who stated that the circulation of solid granules that occur in a fluidization reactor can enable heat transfer to occur without significant obstacles. Therefore it is still necessary to develop several research variations related to this fluidized system.



### 3.3 Visual Characteristics of Babble at Pressure 8 Bar

The flow visual shows the actual conditions in a fluidized bed reactor chamber at an air pressure of 8 bar, the fluid flow fluctuations that occur are caused by air pressure originating from the compressor.

Fig. 4 is a visual photo of particle fluctuations in the reactor, which can be seen in Fig. 4(a) that air bubbles rise to the top reactor surface starting from the 3<sup>rd</sup> second, meaning that new bubbles are formed and seen in the 3<sup>rd</sup> second which appears in the reactor as black spherical cavity forming two layers hollow surface filled with air near the top surface, but you can also see the surface of silica particle spreading as result of the uneven air pressure in the reactor chamber. On the other hand, in Fig. 4(b), the air pressure that rises at 6 seconds starts in the middle of the reactor, where the distribution of air produced is even in the reactor, even though it looks a bit asymmetrical.

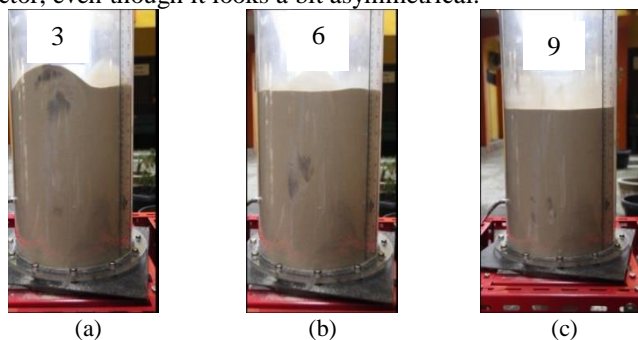


Fig. 4. Visual photographs of bubble fluctuations at pressure 8 bar. a) Visual babble at second 3. b) Visual babble at second 6. c) Visual babble at second 9.

The air pressure in Fig. 4(b) can be seen forming a cavity in the middle reactor and its size is smaller when compared to Fig. 4(a), this condition is due to the increasing time for fluctuations to form, so the formation of air bubble become more constant in each test. The next analysis can be seen in Fig. 4(c), namely the phenomenon formation of fluctuations in air pressure, if seen by the naked eye there are differences in the results and the formation of bubbles, whereas in the previous image, the resulting air bubble still fluctuates, this is because time not long. Fig. 4(c) shows constant visual as seen on the surface of the reactor which is filled with silica particles that have been evenly distributed as well as the bubble cavities that are no longer visible. Data from observations and recorded measurements of the average temperature the reactor obtained the highest was 29.05°C using silica sand material as fuel with the time of taking data for rising bubble starting at 3<sup>rd</sup> second, 6<sup>th</sup> second, and 9<sup>th</sup> second. The height of the silica sand material in this experiment was 25 cm which was measured from the bottom of the hole plate before being given air pressure. After being given air pressure from the compressor, the bed height increased to 29.7 cm, while for the diameter of the bubble produced in the 9<sup>th</sup> second, the average was  $\varnothing = 2.7$  cm. and a 28.4 cm stretch of silica sand.

### 3.4 Analysis of Bubble Formation with Babble Size

Fig. 5 shows that the bubble formation time with the babble size produced in this research is fluctuating for each air pressure variation. At an input air pressure of 4 bar, the time of bubble formation increases at the 3<sup>rd</sup> second, 6<sup>th</sup> second and, 9<sup>th</sup> second and is seen to continue to decrease with each increase in input air pressure. The decrease in babble diameter in each input air pressure increase is caused by several factors such as friction, collisions between particles, and particle type. The formation of air bubbles in the fluidized bed reactor starts at 3<sup>rd</sup> second where this condition applies to all air pressure input sourced from the compressor.

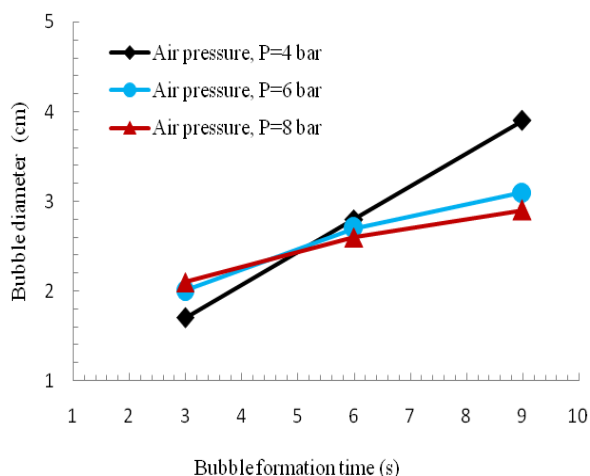


Fig. 5. Graph of the relationship between bubble formation time with babble size produced.

### 3.5 Analysis Air Pressure Input with Resulting Babble

The next analysis and discussion is in Fig. 6, which shows the air pressure input from the compressor with the resulting babble size for each air pressure of 4 bar, 6 bar and 8 bar. At pressure of 4 bar, a bubble diameter of 1.7 cm is obtained and seen to continue to increase with the peak of 3.9 cm. Fig. 6 also shows that at the pressure of 6 bar, the highest diameter of 3.1 cm is obtained, namely the blue line, while for the pressure of 8 bar, the diameter of the babble is 2.9 cm. The research results that have been converted into real data provide information that the greater the air pressure entering the reactor, the smaller the babble diameter.

From the graph in Fig. 6, it can also be seen that the size of bubble diameter produced is the largest at an air pressure of 4 bar, on the other hand, the smallest bubble size is obtained at the highest air pressure, namely when the input air pressure is 8 bar. When considering this phenomenon, it can be concluded that the greater air pressure from the compressor injected into the reactor with the formation of the same bubble fluctuation, results of the largest babble diameter size are obtained at the lowest pressure, which in this case is 4 bar, this condition is because low-pressure results in the push of air into particle material also small or not yet optimal so that the fluctuation air bubble that spread to the expanse of large cavity particle. The treatment applies vice versa, namely when air pressure from the compressor is increased, the size of bubble formed also gets smaller, this condition is because the large air pressure makes it easier to penetrate the silica particle material so that the air bubble that spreads to the particle bed become smaller.

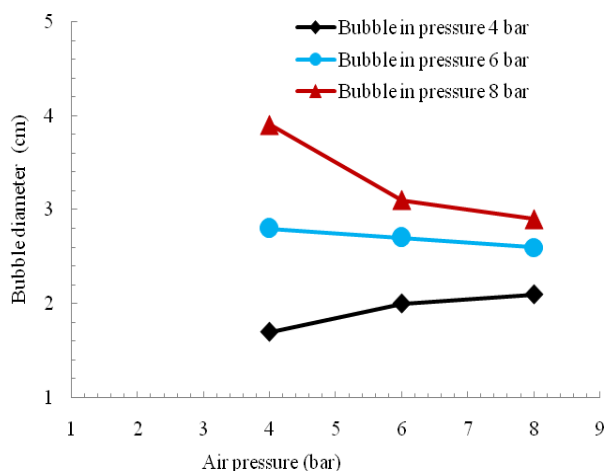


Fig. 6. Graph of the relationship between air pressure with the resulting babble size.

This result condition is also confirmed in the research of C. Zhang et. al. in 2017 and M. Jahandar et. al. which was produced in 2022 and explains the process of increasing non-uniform fluidized air bubbles occurring in the inner fluidized layer, resulting in sections of large bubbles in a non-uniform situation, so it is necessary to adjust the pressure distribution of the air injected into the reactor chamber. On the other hand, the buildup of particulate material on the walls of the reactor which is getting denser due to hardening due to mixing with wet air, makes the formation of air bubbles take longer to reach the peak point of the bubble.

### 3.6 Analysis Air Pressure Input with Fluidized Bed Reactor Temperature

The air pressure that enters the fluidized bed reactor greatly affects the final result of the characteristic of air bubble. This research also measures the temperature in the reactor to obtain information regarding temperature phenomena at the bottom reactor and the upper surface of reactor which is limited by silica particle material. A thermocouple is a measuring instrument installed to obtain this information. Fig. 7 shows that for every given increase in air pressure input with pressure variation from 4 bar, 6 bar and 8 bar, there tends to be an increase in temperature. T1 is the black line in Fig. 7 which is the temperature placement thermocouple at the bottom or at the bottom reactor while T2 is shown as the red line, namely the placement thermocouple at the top or slightly below the top surface of particle material, approximately 15 cm from the top surface material particle. The results of measurements that have been processed and made into a graphical image show that for the bottom temperature of 4 bar, an average temperature of 25.45°C is obtained. At the input air pressure of 6 bar, an average temperature of 27.75°C is obtained, while the highest temperature is at pressure 8 bar, which is 29.05°C so that in this study it can be concluded that the greater air pressure, the greater the friction between the particles. With the reactor wall, between the particles and the particles themselves eventually, moisture also forms and increases the temperature to be hotter.

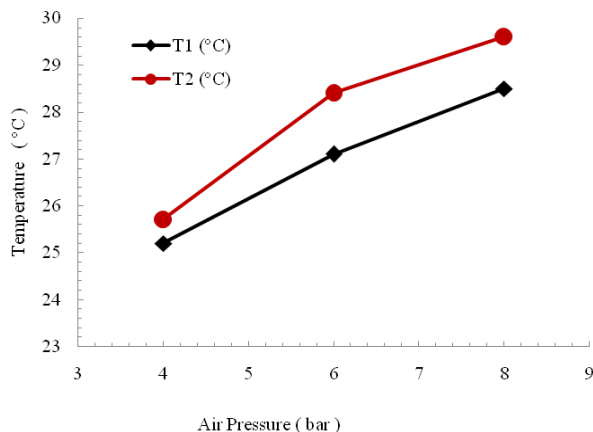


Fig. 7. Graph of the relationship between air pressure input and fluidized bed reactor temperature.

### 3.7 Particle Size Analysis with Minimum Fluidization Velocity

Fig. 8 shows the phenomenon of average particle size with the fluidization velocity in the reactor chamber which is seen theoretically and experimentally, where it can be seen that the purple line theoretically visible data based on existing references, indicating that the average particle size continues to increase with input air pressure and likewise the speed of flowing air also getting faster with the value in this data being respectively 0.05 m/s, 0.19 m/s and 0.49 m/s. on the other hand, where you can see the dotted graphic line, each in black, blue and red, is the result of research that has been carried out in the fluidized bed reactor room. In the figure, it can be seen that all lines show an increase

phenomenon which of course has different values, all of which are influenced by input air pressure that is introduced into the fluidized bed reactor chamber.

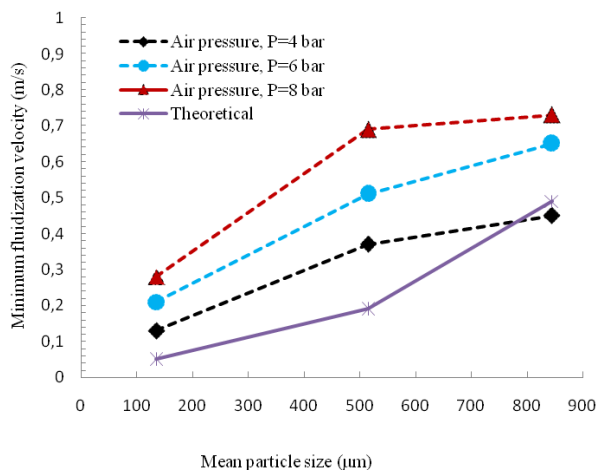


Fig. 8. Graph of the relationship between average particle size with minimum velocity fluidization in fluidized bed reactor.

The average size of silica particles at 4 bar is 135 µm with a fluidization velocity of 0.45 m/s. The next discussion is for the pressure condition of 6 bar, namely the average particle size of 515 µm is obtained with a fluidization velocity of 0.65 µm while the fluidization velocity with an input air pressure of 8 bar is 0.73 m/s. These conditions and phenomena illustrate that air pressure is the main part that must be considered, especially in a fluidized system, in this case, for example, regulating the intake of air to the reactor and constant conditioning of the incoming air in a fluidized bed reactor so that the process becomes perfect.

The smaller the air pressure entering the fluidized bed reactor chamber, the longer the time until the airflow to the tip reaches maximum bubbles, the impact of which is that the desired uniform process of air bubbles will also not be as expected. However, on the other hand, if the air pressure of the fluidized is given a large amount, the air bubbles will form more quickly together.

## 4 Conclusion

Research related to the fluidization system using a fluidized bed reactor has been carried out, where the number of holes 8 in the bed section gives the result that the characteristics of air bubbles produced from the fluidized system process can fluctuate continuously, this condition is influenced by the amount of air pressure input provided through the compressor. The characteristic size of the air bubble the size of air bubble becomes smaller if the air pressure entering into the fluidized bed reactor is greater, where the largest size is 3.9 cm in diameter while the smallest is 2.9 cm. This result is obtained from the increase in bubbles at the 9<sup>th</sup> second. In addition, the average temperature in the fluidization chamber is 29.05°C, where the temperature conditions illustrate that the characteristics in the reactor chamber will be faster, the constant fluctuation of bubble produced if the temperature is higher and vice versa in a fluidized system.

## Acknowledgment

We would like to thank the Universitas Negeri Medan for providing funding support for the smooth running of this research and also the mechanical engineering department for providing equipment during the research process at the workshop.

## References

- [1] S. Yu, X. Yang, J. Xiang, H. Zhou, Q. Li, Y. Zhang, "Effects of bed size on the voidage in gas-solid bubbling fluidized beds", *Powder Technology*, Volume 387, pp. 197-204, 2021. <https://doi.org/10.1016/j.powtec.2021.04.035>

- [2] J. Oshitani, S. Kato, T. Tsuji, K. Washino, S. Harada, H. Kajiwara, K. Matsuoka, G. V. Franks, "Influence of air velocity and powder bed height on local density and float-sink of spheres in a gas-solid fluidized bed", *Advanced Powder Technology*, Volume 34, Issue 9, pp.1-8, 2023. <https://doi.org/10.1016/j.apt.2023.104146>.
- [3] J. Oshitani, T. Sasaki, T. Tsuji, K. Higashida, D.Y.C. Chan, "Anomalous sinking of spheres due to local fluidization of apparently fixed powder beds", *Phys. Rev. Lett.* Vol.116, issue.6, 2016. <https://doi.org/10.1103/PhysRevLett.116.068001>
- [4] K. Higashida, K. Rai, W. Yoshimori, T. Ikegai, T. Tsuji, S. Harada, J. Oshitani, T. Tanaka, "Dynamic vertical forces working on a large object floating in gas-fluidized bed: discrete particle simulation and Lagrangian measurement", *Chem. Eng. Sci.* vol.151, pp.105-115, 2016. DOI:10.1016/j.ces.2016.05.023
- [5] Z. Fu, J. Zhu, S. Barghi, Y. Zhao, Z. Luo, C. Duan, "The distribution of bed density in an air dense medium fluidized bed with single and binary mixtures of Geldart B and/or D particles", *Miner. Eng.* Vol.142, 2019. <https://doi.org/10.1016/j.mineng.2019.105926>
- [6] W. Yoshimori, T. Ikegai, K. Uemoto, S. Narita, S. Harada, J. Oshitani, T. Tsuji, H. Kajiwara, K. Matsuoka, "Non-invasive measurement of floating-sinking motion of a large object in a gas-solid fluidized bed", *Granul. Matter* 21, 42, 2019. <https://doi.org/10.1007/s10035-019-0897-3>
- [7] J. Oshitani, T. Sasaki, T. Tsuji, S. Harada, H. Kajiwara, K. Matsuoka, "Unstable sinking of spheres at higher air velocity in a gas-solid fluidized bed", *Adv. Powder Technol.* Vol.32, issue.4, pp.1300-304, 2021. <https://doi.org/10.1016/j.apt.2021.02.021>
- [8] F. Xuchen, R. Yongxin, D. Liang, Z. Chenyang, Z. Yuemin. "Optimization of coal size for beneficiation efficiency promotion in gas-solid fluidized bed", *Particulate Science and Technology*. Vol.41. pp.1-12, 2022. DOI:10.1080/02726351.2022.2061393.
- [9] L. Wei., Y. Lu., Jiang, G., Hu, J., J. Zhu, "Unsteady-state bubble dynamic wave velocity of gas-solid bubbling fluidized bed", *Chemical Engineering Research and Design*, vol.126, pp.1-10, 2017. <https://doi.org/10.1016/j.cherd.2017.08.013>
- [10] X. Li, M. Liu, Y. Li, "Bed expansion and multi-bubble behavior of gas-liquid-solid micro-fluidized beds in sub-millimeter capillary", *Chemical Engineering Journal*, vol.328, pp.1222-1138, 2017. <https://doi.org/10.1016/j.cej.2017.07.107>
- [11] B. Zhang, Y.M. Zhao, Z.F. Luo, S.L. Song, G.M. Li, S. Cheng, "Utilizing an air-dense medium fluidized bed dry separating system for preparing a low-ash coal", *Int. J. of Coal Prep. and Util.*, vol.34, issue.6, pp. 285-295, 2014. <https://doi.org/10.1080/19392699.2014.880695>
- [12] H.C. Su, Y.L. Liu, Z.L. Tian, S. Zhang, A.M. Zhang, "Coupling between a bubble and a liquid-liquid interface in viscous flow", *Int. J. Multiph. Flow*, Vol. 160, 2023. <https://doi.org/10.1016/j.ijmultiphaseflow.2022.104373>
- [13] Y. Honda, S. Saito, T. Anzai, S. Harada, T. Tsuji, K. Washino, J. Oshitani, H. Kajiwara, K. Matsuoka, "Experimental verification of the Brinkman equation around objects with various shapes in gas-solid stationary and fluidized beds", *Int. J. Multiph. Flow*, vol.160, 2023. <https://doi.org/10.1016/j.ijmultiphaseflow.2022.104359>
- [14] J. Xiang, Q. Li, Z. Tan, Y. Zhang, "Characterization Of The Flow In A Gas-Solid Bubbling Fluidized Bed by Pressure Fluctuation", *Chemical Engineering Science*, vol.174, pp.93-103, 2017. <https://doi.org/10.1016/j.ces.2017.09.001>
- [15] G. Zhu, B. Zhang, P. Zhao, C. Duan, Y. Zhao, Z. Zhang, G. Yan, X. Zhu, W. Ding, Z. Rao, "Upgrading low-quality oil shale using high-density gas-solid fluidized bed", *Fuel*, Volume 252, pp.666-674, 2019. <https://doi.org/10.1016/j.fuel.2019.03.140>
- [16] L. Junyu, W. Dan, Q. Jinpeng, D. Chenlong, "On the dynamics of a sinking object in a bubbling gas-solid fluidized bed by a ball-type inertial measurement unit and electrical capacitance tomography", *Powder Technology*. Vol.411, 2022. DOI:10.1016/j.powtec.2022.117908.
- [17] C. Zhang, P. Li, C. Lei, W. Qian, F. Wei, "Experimental study of non-uniform bubble growth in deep fluidized beds", *Chemical Engineering Science*, vol.176, pp.515-523, 2017. <https://doi.org/10.1016/j.ces.2017.10.006>
- [18] M. Jahandar Lashaki, A. A. Sarbanha, S. Movahedirad, "Overall particles flow pattern in a two-zone gas-solid fluidized bed with a secondary-gas stream", *Chemical Engineering Research and Design*, Vol.187, pp. 570-583, 2022. <https://doi.org/10.1016/j.cherd.2022.09.023>
- [19] Y. Mao, L. Dong, Y. Dong, W. Liu, J. Chang, S. Yang, Z. Lv, P. Fan, "Fast co-pyrolysis of biomass and lignite in a micro fluidized bed reactor analyzer", *Bioresource Technology*, Volume 181, pp.155-162, 2015. <https://doi.org/10.1016/j.biortech.2015.01.066>
- [20] E.C. Pleite, F. H. Jiménez, L.M. Gutierrez, A.A. Iborra, "Experimental study on the motion of solids around an isolated bubble rising in a vertically vibrated fluidized bed", *Chemical Engineering Journal*, vol.330, pp.120-133, 2017. <https://doi.org/10.1016/j.cej.2017.07.072>
- [21] L. Sang, T. Nan, A. Jaber, J. Zhu, "On the basic hydrodynamics of inverse liquid-solid circulating fluidized bed downer", *Powder Technology*, Volume 365, Pages 74-82, 2020. <https://doi.org/10.1016/j.powtec.2019.04.021>
- [22] C. Mandviwala, J. Gonzalez-Arias, T. B. Vilches, M. Seemann, H. Thunman, "Comparing bed materials for fluidized bed steam cracking of high-density polyethylene: Olivine, bauxite, silica-sand, and feldspar", *Journal of Analytical and Applied Pyrolysis*, Volume 173, 2023. <https://doi.org/10.1016/j.jaap.2023.106049>
- [23] P. Skopec, J. Hrdlika, M. Vodia, "Dry additive desulfurization in oxyfuel bubbling fluidized bed combustor", *Fuel*, Volume 283, 2021. <https://doi.org/10.1016/j.fuel.2020.118945>
- [24] A. Alamri, J. McDonough, V. Zivkovic, "Fluidisation behaviour and wall effects of cohesive hydrotalcite powder in a micro-fluidised bed", *Powder Technology*, Volume 415, 2023. <https://doi.org/10.1016/j.powtec.2022.118192>
- [25] Y. Zhang, "Process intensification in micro-fluidized bed systems: a review", *Chem. Eng. Process. Process Intensif.*, 164, 2021
- [26] S. Geng, "Conditioning micro fluidized bed for maximal approach of gas plug flow", *Chem. Eng. J.*, 351, pp. 110-118, 2018
- [27] Y. Guo, "Development of a multistage in situ reaction analyzer based on a micro fluidized bed and its suitability for rapid gas-solid reactions", *Energy Fuel*, 30 (7), pp. 6021-6033, 2016.
- [28] C.R.K. Windows-Yule, S. Gibson, D. Werner, D.J. Parker, T.Z. Kokalova, J.P.K. Seville, "Effect of distributor design on particle distribution in a binary fluidised bed", *Powder Technology*, Volume 367, Pages 1-9, 2020. <https://doi.org/10.1016/j.powtec.2020.03.034>